Direct Formation of Quasimolecular $1s\sigma$ Vacancies in Uranium-Uranium Collisions*

Wilfried Betz, Gerhard Soff, Berndt Müller, and Walter Greiner
Institut für Theoretische Physik der Johann Wolfgang Goethe-Universität, Frankfurt am Main, Germany
(Received 14 June 1976)

The direct (Coulomb) formation of electron vacancies in the $1s\sigma$ state of superheavy quasimolecules is investigated for the first time. Its dependence on the impact parameter, projectile energy, and its contribution from excitations into the continuum and higher bound states are determined.

The fundamental interest in the formation of quasimolecular electron states in heavy-ion collisions centers around two points: (1) It has been possible to observe radiative transitions between the quasimolecular states; particularly the molecular K x rays.[1] With further improvement of the experimental methods and their extension to heavier systems, a systematic spectroscopy of superheavy quasimolecules and even superheavy elements can be envisaged.[2] (2) For $Z=Z_1+Z_2>172$, the conceptually new phenomenon of spontaneous pair creation due to the decay of the neutral electron-positron vacuum in electric fields has been predicted.[3,4] If such overcritical fields occur during the collision of, e.g., U with U, the "decay of the neutral vacuum" furnishes a new fundamental test of quantum electrodynamics which also serves as a prototype for similar processes in all areas of the physics of very strong fields and strong binding.

The common feature of these two classes of experiments is the necessary vacancy production in the $1s\sigma$ quasimolecular states. Unfortunately, very little is known about the formation of $1s\sigma$ vacancies, because the well-understood promotion mechanism is not applicable and the continuum is expected to play an important role. Existing calculations of continuum ionization[5] are limited to $H+H^+$ (nonrelativistic); their numerical accuracy and agreement with experimental heavy-ion data[6] are poor. Estimates[6-8] for the vacancy formation in U-U collisions of ca. 1500 MeV lab energy range from 4×10^{-6} to 10^{-1}.

To calculate the quasimolecular $1s\sigma$ vacancy formation amplitude during and after the collision, we start from the instantaneous, stationary solutions of the two-center Dirac equation[9]

$$\left[\vec{\alpha}\cdot\vec{p}+\beta m_e-\frac{z_1e^2}{|\vec{r}-\vec{R}/2|}-\frac{z_2e^2}{|\vec{r}+\vec{R}/2|}-E_n\right]\varphi_n(\vec{r},\vec{R})=0. \tag{1}$$

We then expand the solution of the time-dependent Schrödinger equation into these basis states and the correspondent occupation amplitudes:

$$\psi(\vec{r},t)=\sum_n a_n(t)\varphi_n[\vec{r},\vec{R}(t)]\exp[-i\int^t dt'\,E_n(t')]. \tag{2}$$

In first-order perturbation theory the amplitudes $a_n(t)$ are given by

$$a_n(t)=-a_n^P\int_{-\infty}^t dt'\langle\varphi_n(t')|\,\partial/\partial t'\,|\varphi_{1s\sigma}(t')\rangle\exp[i\int^{t'}dt''(E_n-E_{1s\sigma})]. \tag{3}$$

Here a_n^P is a constant amplitude (mostly 0 or 1) that shows to what extent the transition $1s\to n$ is allowed by the Pauli principle. In perturbation theory, unitarity is violated to the order $\Delta p=\sum_n a_n^2$, where n runs over all excited states. In an actual U+U collision the $2s\sigma$ and $3s\sigma$ states will be filled, so that in general $a_{2s\sigma}^P=a_{3s\sigma}^P=0$. Under these conditions we find $\Delta p\sim0.1$, which is a measure of the relative error we make using Eq. (3) to solve the scattering equation. If we set, e.g., $a_{2s\sigma}^P=1$ in a fictitious experiment, we find $p\sim0.5$ which shows that a true coupled-channel calculation would be necessary in such an academic situation. It should be stressed that Eq. (3) is not a kind of "never come back" approximation because it allows for oscillations in the excitation amplitude $a(t)$ which indicates a "jumping" of the vacancy between the $1s\sigma$ and the n state until it approaches the final value $a(t=\infty)$ after the collision.

In the corotating coordinate system one can split the translation matrix element into a radial and rotational part:

$$\partial/\partial t\to\dot{R}\partial/\partial R-i\dot{\vec{\theta}}\cdot\vec{J}. \tag{4}$$

For symmetric collisions the rotational part couples to the $3d\pi$ state as lowest state and

—most important—the corresponding matrix element vanishes for $R \to 0$. On the other hand, the radial part couples to all $ns\sigma$, $nd\sigma$, etc. states with large matrix elements $\langle ns\sigma | \partial/\partial R | 1s\sigma \rangle$ at close distances. We have therefore limited our basis to the $1s\sigma$, $2s\sigma$, $3s\sigma$, $4s\sigma$ bound states and the $Es\sigma$ continuum states. For bound state wave functions[10] we have taken the solutions of the one-electron two-center Dirac equation (1). The calculation of the radial matrix elements can be obtained by use of

$$\dot{R}\langle \varphi_n | \partial/\partial R | \varphi_m \rangle = \dot{R}(E_m - E_n)^{-1} \langle \varphi_n | \partial V_{tc}/\partial R | \varphi_m \rangle, \quad (5)$$

from the two-center potential V_{tc}, provided the two wave functions are orthogonal and eigenfunctions of the same Hamiltonian. The matrix elements between bound states as obtained from Eq. (5) are shown in Fig. 1(a) (dashed lines). Between neighboring states, e.g., $1s$-$2s$, $2s$-$3s$, $3s$-$4s$, etc. they are almost equal. Hence only the matrix elements with the $1s\sigma$ state are shown. They do not vanish for large separations R but approach a constant value. This is known to be due to the fact that the molecular states $\varphi_n(R)$ are not asymptotic solutions of the scattering equation, but rather states $\bar{\varphi}_n(R) = \varphi_n(R) \exp[-(i/2)m_e \vec{v} \cdot \vec{r}]$

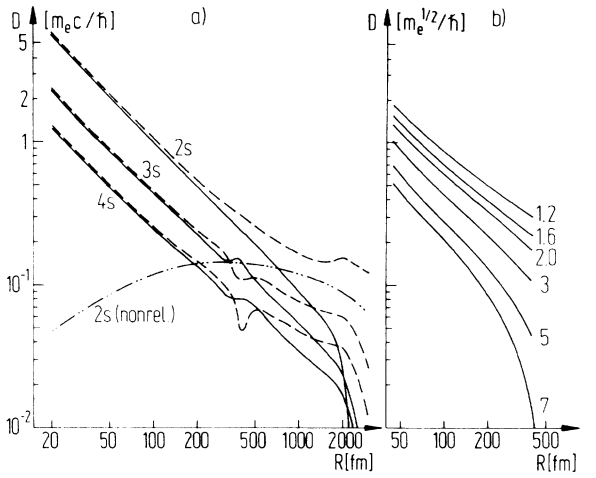

FIG. 1. (a) Radial coupling matrix elements of the $1s\sigma$ to the $2s\sigma$, $3s\sigma$, $4s\sigma$ levels in U+U as a function of internuclear separation. The dashed lines are without the translation factor, the full lines are with it. The dash-dotted line shows a nonrelativistic $1s\sigma$-$2s\sigma$ matrix element scaled to U+U. (b) The radial coupling elements of the $1s\sigma$ level to the continuum states (energies in electron masses). The continuum states have been calculated in the monopole approximation.

should be used.[11] Including this "translation factor" in first order in the projectile velocity $\vec{v}$ one finds that the matrix element (5) must be replaced by[12]

$$\dot{R}\left\langle \bar{\varphi}_n \left| \frac{\partial}{\partial R} \right| \bar{\varphi}_m \right\rangle = \dot{R}\left[\left\langle \varphi_n^{(+)} \left| \frac{\partial}{\partial R} \right| \varphi_m^{(+)} \right\rangle - \frac{m_e}{2}(E_m^{(+)} - E_n^{(-)}) \langle \varphi_n^{(-)} | z | \varphi_m^{(+)} \rangle \right], \quad (6)$$

where $\varphi_n^{(-)}$ denotes the molecular state of negative parity (e.g., $2p_{1/2}\sigma$) which in the separated atomic limit corresponds to the positive parity state $\varphi_m^{(+)}$ (e.g., $1s\sigma$). z is the intrinsic coordinate along the molecular axis. The matrix elements (6) are shown in Fig. 1(a) by solid lines. They vanish rapidly beyond $R = 2000$ fm, indicating the point where the two K shells just begin to influence each other.

The most noteworthy feature of the matrix elements is, however, the steep increase even at very small R. For comparison we have scaled a nonrelativistic matrix element to U+U [dash-dotted line in Fig. 1(a)]. The difference is due to the fact that for $Z_1 + Z_1 > 137$ the relativistic $ns\sigma$ and $np_{1/2}\sigma$ wave functions are extremely sensitive on R, especially for small separations[3,4,9] (this is the lack of a "runway" in the correlation diagram). The smooth behavior of the matrix elements suggested calculating them also in the monopole approximation, substituting a blown-up nucleus of radius $\frac{1}{2}R$ for the two nuclei. The results are in agreement within 2% of the exact curves in the range $20 \text{ fm} \leq R \leq 400$ fm. This justifies one to calculate the radial matrix elements to the $Es\sigma$ continuum states in the monopole approximation [for both states in order for Eq. (5) to remain valid] as shown in Fig. 1(b). The total transition strength into the continuum,

$$|D_{cont}|^2 = \int_{m_e}^{\infty} dE \, |\langle Es\sigma | \partial/\partial R | 1s\sigma \rangle|^2, \quad (7)$$

is larger than into the $2s\sigma$ bound state, $|D_{2s\sigma}|^2$. For the bound states we find $|D_{ns\sigma}|^2 \cdot n^4 \sim \text{const}$, i.e., the summation is rapidly convergent. This behavior implies that the energy density of ns states is $dE/dn \sim n^{-4}$ in the $Z = 184$. Indeed we find from numerical calculations that $E_{ns} \sim n^{-\gamma}$ with $\gamma \sim 2.7$ ($E_{ns} \sim n^{-2}$ in the hydrogen atom). We conclude that the radial coupling does not exhibit an anomalous threshold behavior toward the continuum.

The complex amplitudes $a_n(t)$ are now obtained by numerical integration of Eq. (3) along classi-

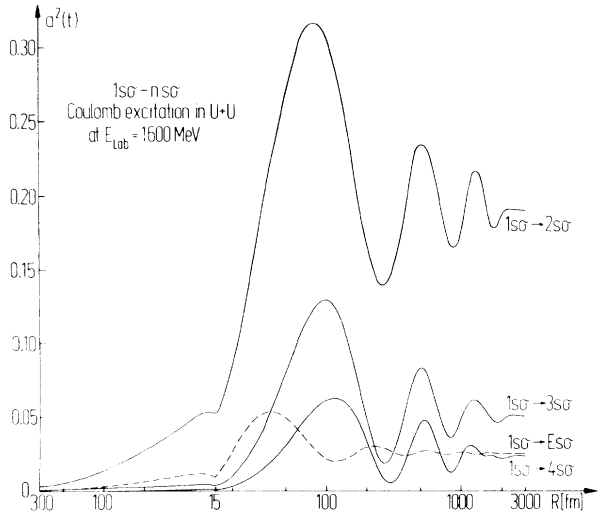

FIG. 2. Total probability for Coulomb excitation of a $1s\sigma$ electron in U+U into a vacant $ns\sigma$ level and into the continuum ($Es\sigma$) at zero impact parameter. One-step and multistep channels are included. The strong increase sets in just after the point of closest approach.

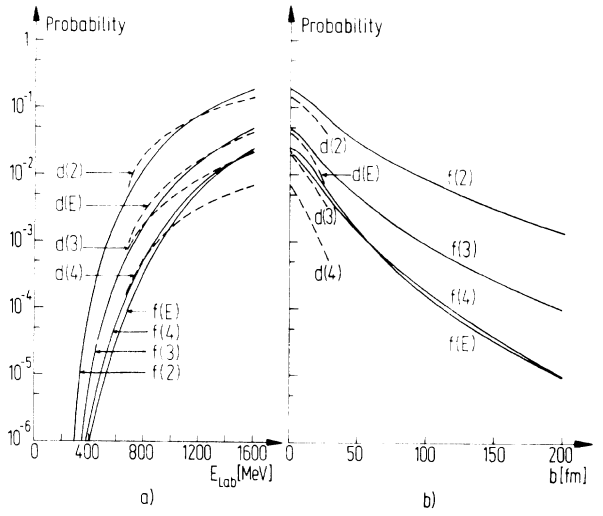

FIG. 3. (a) Energy dependence of the Coulomb ionization of the U+U $1s\sigma$ level at zero impact parameter. Excitation into the $2s\sigma$, $3s\sigma$, $4s\sigma$ states and the continuum (E) is shown separately. $f(n)$ denotes the final atomic ionization probability; $d(n)$ the average probability over the region where the $1s\sigma$ state has dived into the negative energy continuum. (b) Impact parameter dependence of the Coulomb ionization of the $1s\sigma$ level at $E_{lab} = 1600$ MeV. Notations are as in (a).

cal Coulomb trajectories for the heavy ions. For excitation into the $2s\sigma$ and $Es\sigma$ states this is straightforward, whereas for the $3s\sigma$ and $4s\sigma$ states a number of channels add up coherently (e.g., the one-step excitation $1s\sigma$-$3s\sigma$ and the two-step process $1s\sigma$-$2s\sigma$-$3s\sigma$).

The total excitation probabilities $|a_n|^2$ and $\int dE\,|a_E|^2$ are shown in Fig. 2 as a function of R, under the assumption that the final state is vacant. As expected, the curves show oscillations with a maximum twice as high as the final excitation probability $P(b)$. The steep rise of $|a(t)|^2$ just beyond the distance of closest approach can easily be understood. During the approach a major portion of the $1s\sigma$ electronic density flows inward following the motion of the nuclei. When this motion is suddenly reversed the electron is left behind and redistributes over other states. This acceleration process weakens quickly for high impact parameters, as is seen in Fig. 3(b). The excitations into the continuum, i.e., ionization, vary also over the trajectory: After the collision they are comparable to excitation into the $4s$ state (which will be practically vacant from simple velocity arguments), whereas in the region where the $1s\sigma$ state of U+U has dived into the positron continuum ($R \lesssim 35$ fm) they are dominant (see Fig. 3). The projectile energy dependence of excitation is shown in Fig. 3(a), the impact parameter dependence in Fig. 3(b). The final excitation after the collision is denoted by $f(n)$, the average excitation over the diving region by $d(n)$. To obtain cross sections, the numbers must be multiplied by a factor of 2 for the two-spin $1s\sigma$ states. For example, at 1600 MeV and zero impact parameter the probability to have a $1s\sigma$ vacancy in the diving region is predicted to be larger than 0.08. This number is crucial for the proposed positron experiment because it is bigger than the value 0.01 which was assumed in previous calculations of the cross sections.[3]

With decreasing incident ion energy the excitation probabilities fall off very steeply, until at tandem energies ($E_{lab} \lesssim 200$ MeV) they are much less than 10^{-6}. The same is true for increasing impact parameters: Typically the probability shrinks to one half at $b = 20$ fm. This will facilitate coincidence experiments, because all the cross section goes into large angle collisions anyway. Figure 3(b) allows also an estimate of the total cross section for atomic K-vacancy production $\sigma_K^{dir} \sim 2$ b, which is very close to the cross section expected from conversion of Coulomb-excited nuclear states.[13] We propose to separate the two mechanisms experimentally by looking at double-K-vacancy production with

$\sigma_{KK}^{dir} \sim 25$ mb. This cannot be caused by conversion because the lifetime of nuclear states is ca. 10^{-11} sec whereas a K vacancy in U lives only for about 10^{-17} sec.

We conclude that the $1s\sigma$-vacancy production in U + U by direct excitation is much larger than expected. The influence of relativity on the behavior of electrons in superheavy quasimolecules is dominant and cannot be accounted for by small "relativistic corrections." These results show that many proposed experiments are possible: The observation of positron production due to spontaneous decay of the vacuum,[3] of molecular x rays[2] from the system Pb + Pb, and the investigation of magnetic fields in the 10^{14} G range,[10] to name only a few.

*Work supported by the Bundesministerium für Forschung und Technologie and by the Gesellschaft für Schwerionenforschung.

[1]R. W. Saris, W. F. van der Weg, H. Tawara, and W. A. Lambert, Phys. Rev. Lett. 28, 717 (1972); P. H. Mokler, H. J. Stein, and P. Armbruster, Phys. Rev. Lett. 29, 827 (1972); W. E. Meyerhof, T. K. Saylor, S. M. Lazarus, W. A. Little, and B. B. Triplett, Phys. Rev. Lett. 30, 1279 (1973); P. Gippner, K. H. Kaun, F. Stary, W. Schulze, and Yu. P. Tretyakov, Nucl. Phys. A230, 509 (1974); C. K. Davis and J. S. Greenberg, Phys. Rev. Lett. 32, 1215 (1974); W. Wölfli, Ch. Stoller, G. Bonani, M. Suter, and M. Stöckli, Lett. Nuovo Cimento 14, 577 (1975).

[2]B. Müller, R. K. Smith, and W. Greiner, Phys. Lett. 53B, 401 (1975).

[3]W. Pieper and W. Greiner, Z. Phys. 218, 327 (1969); B. Müller, H. Peitz, J. Rafelski, and W. Greiner, Phys. Rev. Lett. 28, 1235 (1972); R. K. Smith, H. Peitz, B. Müller, and W. Greiner, Phys. Rev. Lett. 32, 554 (1974).

[4]Ya.B. Zeldovich and V. S. Popov, Usp. Fiz. Nauk 105, 403 (1971) [Sov. Phys. Usp. 14, 673 (1972)].

[5]V. Sethuraman, W. R. Thorson, and C. F. Lebeda, Phys. Rev. A 8, 1316 (1973); W. R. Thorson, Phys. Rev. A 12, 1365 (1975).

[6]W. E. Meyerhof, Phys. Rev. A 10, 1005 (1974).

[7]C. Foster, T. R. Hoogkamer, P. Woerlee, and F. W. Saris, to be published.

[8]D. Burch, W. P. Ingalls, H. Wiemann, and R. Vandenbosch, Phys. Rev. A 10, 1245 (1974).

[9]B. Müller, J. Rafelski, and W. Greiner, Phys. Lett. 47B, 5 (1973); B. Müller and W. Greiner, Z. Naturforsch. 31a, 1 (1976).

[10]J. Rafelski and B. Müller, Phys. Rev. Lett. 36, 517 (1976).

[11]D. R. Bates and R. McCarroll, Proc. Roy. Soc. London, Ser. A 245, 175 (1958).

[12]D. R. Bates and D. A. Williams, Proc. Phys. Soc. London 83, 425 (1964).

[13]V. Oberacker, G. Soff, and W. Greiner, Phys. Rev. Lett. 36, 1024 (1976).

Angular Distribution of Xe $5s \rightarrow \epsilon p$ Photoelectrons: Direct Evidence for Anisotropic Final-State Interaction*

J. L. Dehmer
Argonne National Laboratory, Argonne, Illinois 60439

and

Dan Dill†
Department of Chemistry, Boston University, Boston, Massachusetts 02215
(Received 18 August 1976)

The angular distribution of Xe $5s \rightarrow \epsilon p$ photoelectrons has been measured yielding an asymmetry parameter $\beta = 1.4 \pm 0.1$ at 304 Å. This deviation from the intuitively expected result $\beta = 2$ (for a pure $\cos^2\theta$ distribution) for photoionization of an s subshell of a $^1s_0$ target is a direct manifestation of anisotropic interactions experienced by the electron during the ejection process. The combined effect of interchannel and spin-orbit coupling is proposed as the likely interaction mechanism.

Photoionization of the Xe $5s$ subshell by electric dipole interaction can be written schematically as

$$\mathrm{Xe}(5s^2 5p^6\, {}^1S_0, \pi_0 = +1) + \gamma(j_\gamma = 1, \pi_\gamma = -1) \rightarrow \mathrm{Xe}^+(5s5p^6\, {}^2S_{1/2}, \pi_c = +1) + e^-[ls, \pi_e = (-1)^l]. \quad (1)$$

The orbital momentum l of the photoelectron is restricted by angular momentum balance,

$$\vec{J} = \vec{J}_0 + \vec{j}_\gamma = \vec{J}_c + \vec{s} + \vec{l}, \quad (2)$$

to the range $l \leq 2$. Furthermore, the parity of the photoelectron is $\pi_e = -1$ (odd) because of parity